Control System Design of Self-balanced Bicycles by Control Moment Gyroscope

Article *in* Lecture Notes in Electrical Engineering · January 2015

DOI: 10.1007/978-3-662-46466-3_21

2 authors:

Jiarui He
Tsinghua University
2 PUBLICATIONS **10** CITATIONS
SEE PROFILE

Mingguo Zhao
Tsinghua University
68 PUBLICATIONS **290** CITATIONS
SEE PROFILE

Chapter 21
Control System Design of Self-balanced Bicycles by Control Moment Gyroscope

Jiarui He and Mingguo Zhao

Abstract The unmanned bicycle, as a type of unmanned vehicles, has become a research hotspot recently, and one of the most challenging problems for its realization is the method to keep the bicycle balanced. In this paper, we analyze the dynamic model of self-balanced bicycles using a Control Moment Gyroscope (CMG). The gyroscopic theory shows that by making the spinning flywheel precess, the CMG module generates a moment to resist the gravitational moment and keep the bicycle balanced. According to the gyroscopic theory, we design the mechanical structure and control system of the CMG device and use state feedback control to configure the poles in order to keep the system stable. We obtain the possible feedback coefficient according to the behavior of our system by MATLAB simulations and then adjust the feedback coefficient to get a more stable and robust system through physical experiments. The results of our physical experiments show that the feedback control method can been used to keep the bicycle balanced.

Keywords Balanced · Control system design · Control moment gyroscope · State feedback

21.1 Introduction

Many institutions and enterprises are researching unmanned vehicles and have achieved some significant progress in recent years, unmanned bicycle as a widely used vehicle is a research hotspot. Compared to automobiles, bicycles have more flexibilities due to the small size and more difficulties due to the two-wheeled structure. Bicycles can go through small alleys and other narrow spaces, while

J. He (✉) · M. Zhao
Robot Control Laboratory, Tsinghua Univerisity, Beijing 100084, China
e-mail: hjr13@mails.tsinghua.edu.cn

M. Zhao
e-mail: mgzhao@mail.tsinghua.edu.cn

Z. Deng and H. Li (eds.), *Proceedings of the 2015 Chinese Intelligent Automation Conference*, Lecture Notes in Electrical Engineering 338,
DOI 10.1007/978-3-662-46466-3_21

automobiles cannot. Bicycles will fall down when the forward velocity is very low, while automobiles do not have this problem. Therefore, the first step to design unmanned bicycles is to make the bicycle self-balanced.

The methods to achieve a self-balanced bicycle are mainly classified into four types. The first type is using a control moment gyroscope (CMG); Beznos et al. use gyroscopic stabilization to balance a bicycle in 1998 [1], and Harun Yetkin introduces a sliding mode controller (SMC) to control a CMG in 2014 [2]. The CMG method can provide a large torque, but energy consumption of CMG is very high because the flywheel is spinning all the time. The second type is mass balancing; Getz and Marsden balance the bicycle by swinging a massive ball in 1995 [3], and Masaki Yamakita and Atsuo Utano use a massive balancer to control the bicycle for trajectory tracking in 2005 [4]. The mechanical structure of mass balancing is simple, but the torque this method could provide is small. The third type is steering control; J. Fajans et al. introduce the theory of steering control in the American Journal of Physics in 1999 [5], and Tanaka and Murakami use steering control to achieve the balance of a bicycle in 2004 [6]. The energy consumption of steering control is low, but it cannot balance the bicycle at low forward velocity. The forth type is using a reaction wheel; Murata Manufacturing utilizes a reaction wheel to balance the bicycle and produces the well-known self-balancing robot bicycle called Murata Boy in 2005 [7]. The response time of the reaction wheel is short, and the output torque is limited, so it is suitable for the balance of a small bicycle.

In this paper, the bicycle is massive and its center of mass is high, so we choose CMG method to generate a large torque to balance the bicycle. We design the mechanical structure of self-balanced bicycle based on an electric bicycle as showed in Fig. 21.1, the CMG module is installed in the backseat of bicycle. The detail of CMG module is showed as Fig. 21.2. According to CMG theory, the flywheel is spinning fast and we make the gimbal and flywheel precess with an angular rate; the gimbal will generate a moment to resist the gravitational moment, we can control this moment to keep the bicycle balanced.

Fig. 21.1 Self-balanced bicycle

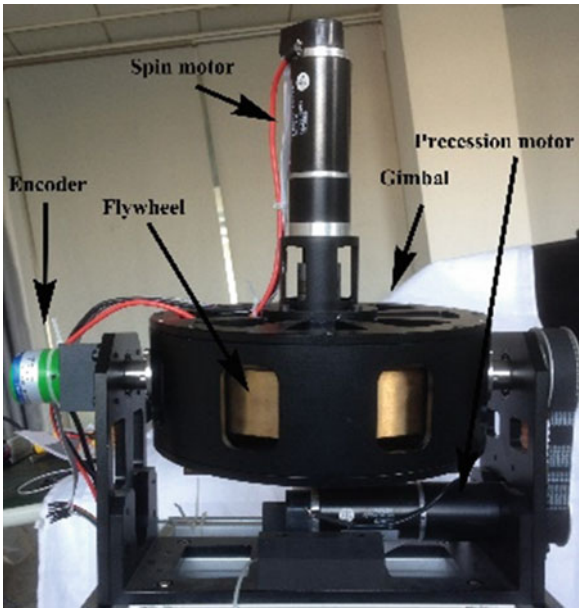

Fig. 21.2 CMG device

The outline of the paper is as follows. In Sect. 21.2, the reference coordinate system is introduced, the dynamic equations are derived. Section 21.3 shows the results of simulations and physical experiments. Section 21.4 presents the conclusion and thoughts about future work.

21.2 Dynamic Model of CMG-Controlled Bicycle

As Fig. 21.3 shows, O_h is a fixed point on the ground, O_g is the geometric center of the gimbal and flywheel. We define three local coordinate systems: horizon coordinate system $O_h - x^h y^h z^h$, bike coordinate system $O_g - x^b y^b z^b$, gimbal coordinate system $O_g - x^g y^g z^g$.

The relative motion of bicycle is consisted of three parts: The body rotates around x^h-axis with lean angle α and lean angular rate $\dot{\alpha}$; the gimbal and flywheel rotate around y^b-axis with precession angle β and precession angular rate $\dot{\beta}$; the flywheel rotates around Z^g-axis with spin angular rate $\dot{\gamma}$.

In order to prevent confusion, we define the part of bicycle excluding the gimbal and flywheel as body. The dynamic model can be divided into two parts: The movement of body, the movement of gimbal and flywheel.

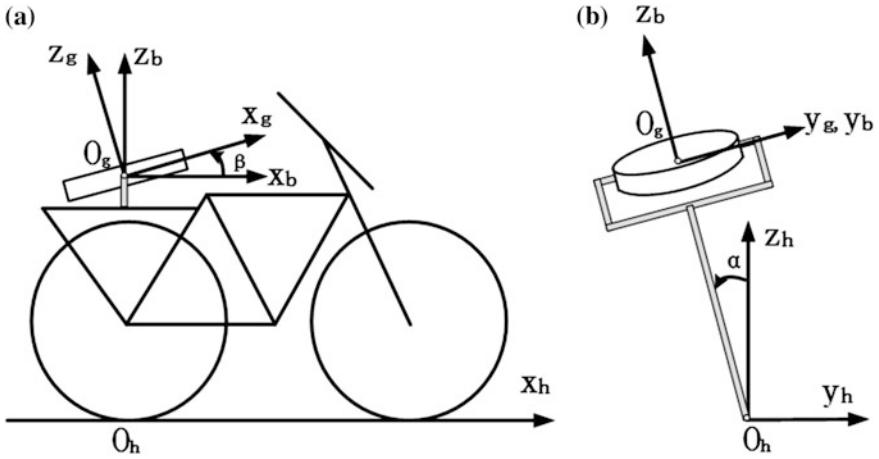

Fig. 21.3 Coordinate systems **a** Side view **b** Front View

21.2.1 The Movement of Body

Ignore the factor of friction, this part has two inputs which have effects on the movement of body. One input is the gravity, another input is the moment τ_b imposed by gimbal in the x^b-axis direction. m_b is the mass of the body, l_b is the height of the body's COG in relation to the ground.

Define generalized coordinates as follows:

$$X_b = \begin{bmatrix} -l_b \sin\alpha \\ l_b \cos\alpha \\ \alpha \end{bmatrix}, F_b = \begin{bmatrix} 0 \\ -m_b g \\ -\tau^b \end{bmatrix}, M_b = \mathrm{diag}(m_b, m_b, I_x^b) \tag{21.1}$$

21.2.2 The Movement of Gimbal and Flywheel

The movement of gimbal and flywheel can be divided into two parts. The first part is that gimbal and flywheel roll around x^h-axis, caused by the torque generated by the gravity. We define that: m_{gf} is the mass of the gimbal and flywheel, l_{gf} is the height of the gimbal and flywheel's COG in relation to the ground. Define generalized coordinates as follows:

$$X_{\mathrm{cmg}} = \begin{bmatrix} -l_{\mathrm{gf}} \sin\alpha \\ l_{\mathrm{gf}} \cos\alpha \end{bmatrix}, F_{\mathrm{cmg}} = \begin{bmatrix} 0 \\ -m_{\mathrm{gf}} g \end{bmatrix}, M_{\mathrm{cmg}} = \mathrm{diag}(m_{\mathrm{gf}}, m_{\mathrm{gf}}) \tag{21.2}$$

The other part is gimbal and flywheel's rolling around y^b-axis and flywheel's rolling around Z^g-axis. The precession motor provides a moment τ_{pre} to drive the

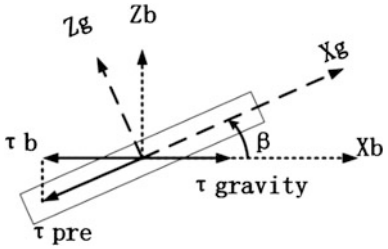

Fig. 21.4 The relation between τ_{rea} and τ_b

gimbal and flywheel to precess, the spin motor provides a moment τ_{spin} to drive the flywheel to spin. Besides, the body give a reaction moment τ_{rea} to the gimbal.

The relation between τ_{rea} and τ_b is showed as Fig. 21.4, τ_b is the component of τ_{rea} in x^g-axis direction, $\tau_{\text{rea}} = \tau_b/\cos\beta$.

We set $O_g - x^g y^g z^g$ as the global coordinate system, so the resultant moment is $\tau = [\tau_b/\cos\beta, \tau_{\text{pre}}, \tau_{\text{spin}}]^T$.

The angular rate of the body ω_b, the angular rate of the gimbal ω_g, the angular rate of the flywheel ω_f, the angular momentum of gimbal, and flywheel H are showed as follows:

$$\begin{aligned}\omega_b &= R_y^{-1}(\beta) \times R_x^{-1}(\alpha) \times [\dot{\alpha}, 0, 0]^T = [\dot{\alpha}\cos\beta, 0, \dot{\alpha}\sin\beta]^T \\ \omega_g &= \left[\dot{\alpha}\cos\beta, \dot{\beta}, \dot{\alpha}\sin\beta\right]^T, \omega_f = \left[\dot{\alpha}\cos\beta, \dot{\beta}, \dot{\alpha}\sin\beta + \dot{\gamma}\right]^T \\ H &= H_p + H_s = I_g\omega_g + I_f\omega_f\end{aligned}$$

where

$$R_x(\alpha) = \begin{bmatrix} 1 & 0 & 0 \\ 0 & \cos\alpha & \sin\alpha \\ 0 & -\sin\alpha & \cos\alpha \end{bmatrix}, R_y(\beta) = \begin{bmatrix} \cos\beta & 0 & -\sin\beta \\ 0 & 1 & 0 \\ \sin\beta & 0 & \cos\beta \end{bmatrix}$$
$$I_g = \text{diag}\left(I_x^g, I_y^g, I_z^g\right), I_f = \text{diag}\left(I_x^f, I_y^f, I_z^f\right)$$

The differential of H is $H_d = I_g\dot{\omega}_g + I_f\dot{\omega}_f + \omega_g \times H_f$. Where $\omega_g \times H_f$ is the moment generated by the precession of gimbal and flywheel.

21.2.3 The Movement of Whole Bicycle

According to Sects. 2.1 and 2.2, we define generalized coordinates as follows:

$$\begin{aligned} q &= [\alpha, \beta, \gamma]^T, X = [X_b, X_{\text{cmg}}, \alpha, \beta, \gamma]^T \\ \text{Left} &= [\text{M}_b\ddot{X}_b; \text{M}_{\text{cmg}}\ddot{X}_{\text{cmg}}; \text{H}_d], \text{Right} = [\text{F}_b; \text{F}_{\text{cmg}}; \tau] \end{aligned}$$

Define $= \frac{\partial X}{\partial q}$, and use $J^T \cdot \text{Left} = J^T \cdot \text{Right}$, we can obtain dynamic equation of bicycle:

$$\begin{bmatrix} \ddot{\alpha}\left[m_{gf}\left(l_{gf}\right)^2 + m_b(l_b)^2 + I_x^b + I_x^f\cos\beta + I_x^g\cos\beta\right] + I_z^f\dot{\beta}\dot{\gamma} + (I_x^f - I_z^f)\dot{\beta}\dot{\alpha}\sin\beta \\ \ddot{\beta}\left(I_y^f + I_y^g\right) - I_x^f\dot{\alpha}^2\cos\beta\sin\beta - I_z^f\dot{\alpha}\cos\beta(\dot{\gamma} - \dot{\alpha}\sin\beta) \\ \ddot{\gamma}I_z^f - \ddot{\alpha}(I_z^f + I_z^g)\sin\beta \end{bmatrix} = \begin{bmatrix} m_{\text{gf}}gl_{\text{gf}}\sin\alpha + m_bgl_b\sin\alpha \\ \tau_{\text{pre}} \\ \tau_{\text{spin}} \end{bmatrix} \tag{21.3}$$

By controlling the spin motor, we can keep $\dot{\gamma}$ to be a constant, $\ddot{\gamma} = 0$ is founded. Linearization of the movement equation around the equilibrium position ($\alpha = \dot{\alpha} = \beta = \dot{\beta} = 0$) yields:

$$\begin{cases} I_x\ddot{\alpha} + H_z\dot{\beta} = H_z\alpha \\ I_y\ddot{\beta} - H_z\dot{\alpha} = \tau_{\text{pre}} \\ I_x\ddot{\gamma}I_z^f = \tau_{\text{spin}} \end{cases}$$

where, $I_x = I_x^b + I_x^f + I_x^g + m_{\text{gf}}l_{\text{gf}}^2 + m_bl_b^2$, $H_z = I_z^f\dot{\gamma}$, $M_x = m_{\text{gf}}\,gl_{\text{gf}} + m_bgl_b, I_y = I_y^f + I_y^g$, $I_z = I_z^f$.

Due to $\ddot{\gamma} = 0$, we can ignore $\ddot{\gamma}I_z^f = \tau_{\text{spin}}$. Letting $x = [\alpha,\ \dot{\alpha},\ \beta,\ \dot{\beta}]^T, \tau_{\text{pre}} = K_ii, K_i$, is torque constant of motor. The state equation of system is given as:

$$\begin{bmatrix} \dot{\alpha} \\ \ddot{\alpha} \\ \dot{\beta} \\ \ddot{\beta} \end{bmatrix} = \begin{bmatrix} 0 & 1 & 0 & 0 \\ \frac{M_x}{I_x} & 0 & 0 & -\frac{H_z}{I_x} \\ 0 & 0 & 0 & 1 \\ 0 & \frac{H_z}{I_y} & 0 & 0 \end{bmatrix}\begin{bmatrix} \alpha \\ \dot{\alpha} \\ \beta \\ \dot{\beta} \end{bmatrix} + \begin{bmatrix} 0 \\ 0 \\ 0 \\ \frac{K_i}{I_y} \end{bmatrix} i = Ax + Bu$$

$$y = \begin{bmatrix} 1 & 0 & 0 & 0 \\ 0 & 0 & 1 & 0 \end{bmatrix}\begin{bmatrix} \alpha \\ \dot{\alpha} \\ \beta \\ \dot{\beta} \end{bmatrix} = Cx \tag{21.4}$$

The rank of controllability matrix is 4, the system is fully controlled. As we all know, the typical indicators of systemic stability is the place of systemic poles.

We can find that two poles of the system are zero, the system is unstable. However, we can use state feedback to configure the poles to keep the system stable:

$$u = i = -kx \tag{21.5}$$

21.3 Simulation and Experiment

To prevent the damage to the instruments, we test the CMG module on an experimental device built by aluminum profiles instead of test on bicycle directly, as is showed in Fig. 21.5. We install an absolute encoder on the ground to test α and $\dot{\alpha}$. The controller is NI-CompactRio-9024, and the reconfigurable embedded chassis is NI-CompactRio-9114.

Define the height of the whole device CoM as l_{dev}, the parameters of experimental device is as Table 21.1.

Substituting the above parameters, the state equation is obtained

$$\begin{aligned} \dot{x} &= \begin{bmatrix} 0 & 1 & 0 & 0 \\ 12.81 & 0 & 0 & -0.55 \\ 0 & 0 & 0 & 1 \\ 0 & 93.98 & 0 & 0 \end{bmatrix} x + \begin{bmatrix} 0 \\ 0 \\ 0 \\ 0.77 \end{bmatrix} u \\ y &= \begin{bmatrix} 1 & 0 & 0 & 0 \\ 0 & 0 & 1 & 0 \end{bmatrix} x \end{aligned} \tag{21.6}$$

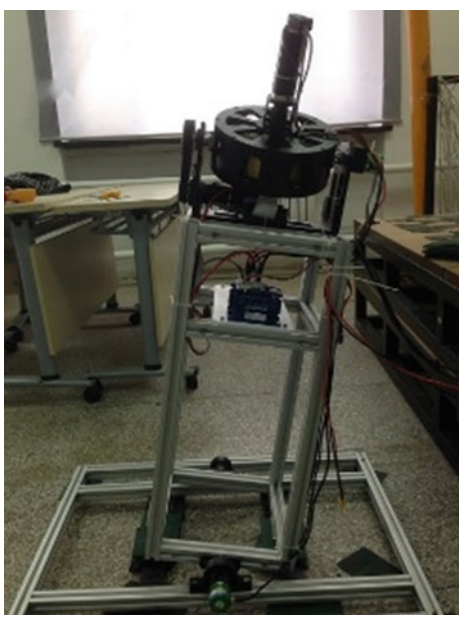

Fig. 21.5 Experimental device

Table 21.1 Parameter values

Parameter	Value	Unit
$[m_f, m_g, m_b]$	[10.513, 6.357, 9.77]	kg
l_{dev}	0.66	m
$[I_x^f, I_y^f, I_z^f]$	[297.98, 297.98, 559.46]	kg × cm^2
I_y^g	782.83	kg × cm^2
I_x	134539.8	kg × cm^2
K_i	0.0603	Nm/A
$\dot{\gamma}$	22.0	r/s

To verify the effect of feedback, we use MATLAB to simulate the behavior of the system. To simplify the complexity of system, we introduce the concept of dominant poles, the dominant poles are located in the specified trapezoidal region and the other poles are located far away from the dominant poles.

The number and place of dominant poles is estimated by simulation and tested by experiment. When we set the poles at $[-50, -1.5, -1.5 + i, -1.5-i]$, the feedback coefficient k is [−2588.7, −506.2, −24.7, 70.7], the states change as Fig. 21.6.

According to the result of simulation, the states approach to the steady state after a few seconds as expected.

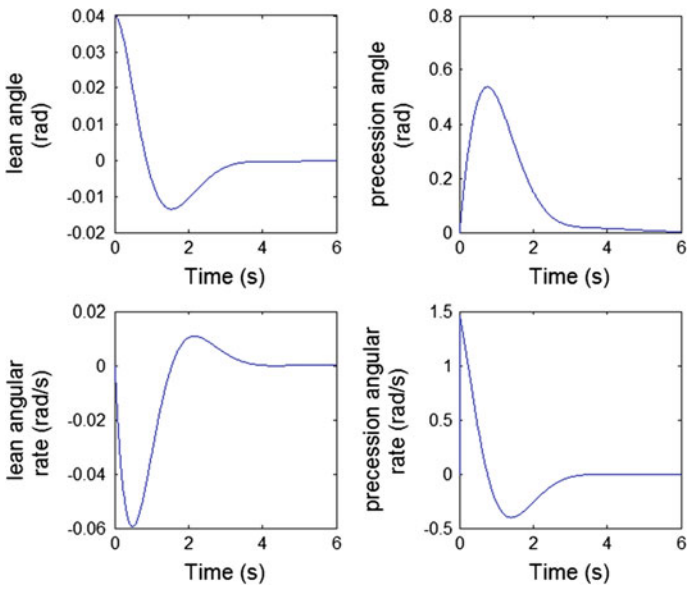

Fig. 21.6 Simulation result

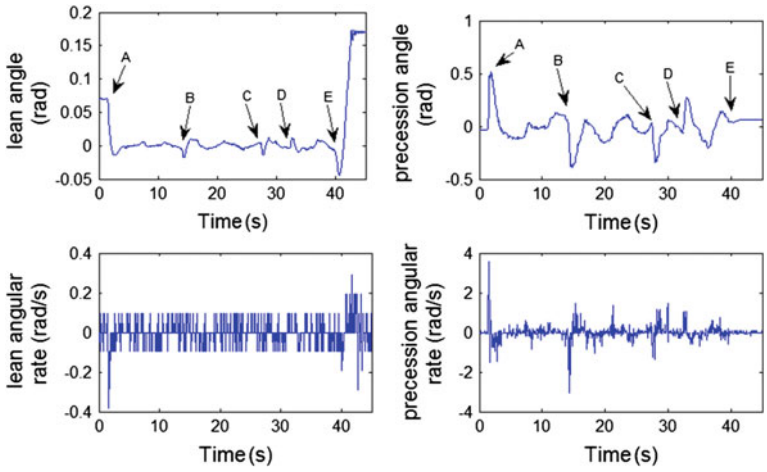

Fig. 21.7 Experiment result

In the experiments, we set the poles the same as simulation parameters, the feedback coefficient k is [−2588.7, −506.2, −24.7, 70.7]. A data collected from the experiment on the CMG device is as Fig. 21.7. The precession motor begin to work at point A, lean angle of point A is 0.0675 rad. After about 3.3 s, the system is running around the steady state. At the points B, C, and D we impose an instant impact on the body, the system deviates from the original state and returns to the steady state. At point E, the precession motor stops working, the device falls down quickly. The result of the experiment shows that feedback control method can been used to keep the bicycle balanced.

21.4 Conclusion and Future Work

To solve the problem that bicycles fall down at low forward velocity, we design state feedback control system to keep the bicycle balanced with a CMG. The results of simulation and physical experiments show that state feedback control can keep the bicycle self-balanced stably and can resist certain instant disturbance.

The first step to make the bicycle balanced is completed by state feedback control. However, the CMG method has some disadvantages; the energy consumption is very high. In addition, since the CMG device imposes a vertical torque $\tau_{rea}\sin\beta$ to the bicycle as shown in Fig. 21.4, the front wheel of the bicycle may leave the ground and the bicycle may even fall backwards. In the future, we will combine steering control with the CMG method to reduce energy consumption and utilize double gyroscopes to eliminate the effect of the vertical torque.

References

1. Beznos AV et al (1998) Control of autonomous motion of two-wheel bicycle with gyroscopic stabilisation. Robot Autom 3:2670–2675
2. Yetkin H et al (2014) Gyroscopic stabilization of an unmanned bicycle. In: American control conference, pp 4549–4554
3. Getz NH, Marsden JE (1995) Control for an autonomous bicycle. Robot Autom 2:1397–1402
4. Yamakita M, Utano A (2005) Automatic control of bicycles with a balancer. In: Advanced intelligent mechatronics, pp 1245–1250
5. Fajans J (2000) Steering in bicycles and motorcycles. Am J Phys 68(7):654–659
6. Tanaka Y, Murakami T (2004) Self sustaining bicycle robot with steering controller. In: Proceedings of 2004 IEEE advanced motion, control confrence 193–197
7. The Murata Boy Website (2005). http://www.murataboy.com/en-global